*Progress In Electromagnetics Research, PIER 93, 255–274, 2009*

# RETRIEVING THE GREEN'S FUNCTION FROM CROSS CORRELATION IN A BIANISOTROPIC MEDIUM

**E. Slob and K. Wapenaar**

Department of Geotechnology
Delft University of Technology (TU Delft)
Stevinweg 1, 2628 CN Delft, The Netherlands

**Abstract**—Development of theory and experiments to retrieve Green's functions from cross correlations of recorded wave fields between two receivers has grown rapidly in the last seven years. The theory includes situations with flow, mechanical and electromagnetic disturbances and their mutual coupling. Here an electromagnetic theory is presented for Green's function retrieval from cross correlations that incorporates general bianisotropic media, which is the most general class of linear media. In the presence of dispersive non-reciprocal media, the Green's function is obtained by cross correlating the recordings at two locations of fields generated by sources on a boundary. The only condition for this relation to be valid is that the medium is non-dissipative. The principle of bianisotropic Green's function retrieval by cross correlation is illustrated with a numerical example.

## 1. INTRODUCTION

The possibility of subsurface imaging using pulse-echo data obtained from cross correlations of noise recordings is known for more than 20 years [1–3]. Over the last seven years much attention has gone to Green's function retrieval from cross-correlations of acoustic ambient noise recordings and to use the results to form acoustic images of the surrounding medium. Weaver and Lobkis [4] retrieved Green's functions from natural thermal field fluctuations. Campillo and Paul [5] applied Green's function retrieval to the diffuse parts of seismic coda waves. Shapiro et al. [6] applied it to surface waves to image the subsurface of California. Draganov et al. [7] retrieved

Corresponding author: E. Slob (e.c.slob@tudelft.nl).

seismic subsurface reflections from noise records. Schuster et al. [8] and Snieder [9] showed with stationary phase theory how not all sources on the boundary play an equally important role, but only those that are stationary for the resulting event. Wapenaar [10] showed that the elastodynamic response of an arbitrary heterogeneous elastic half space can be retrieved from contributions of sources in the subsurface below a pressure free surface. The assumption underlying these formulations and physical experiments, is that the waves travel in lossless, but possibly strongly scattering, media.

Until 2006 no electromagnetic theories and experiments were known, although reports on related subjects exist [11–13] that exploit time-reversal invariance. In dissipative media, time-reversal invariance does not apply at the macroscopic scale. The rigorous incorporation of dissipation in the representations were first reported by Snieder [14], who derived a representation for the scalar diffusion equation, and Slob et al. [15], who derived representations for ground-penetrating radar. Incorporating dissipative media in the formulations leads to an additional volume integral over sources distributed throughout the volume that compensate for the energy loss. At the end of 2006 a general formulation of Green's function retrieval for linear flow, diffusive and wave fields was given by Wapenaar et al. [16]. The configuration where these interferometric representations apply consists of mutually uncorrelated sources on a closed surface enclosing the two receivers.

Interferometric Green's function representations involve cross correlation and integration of recorded fields. This technique extracts the Green's function between two receivers from cross correlation of their recordings and is called interferometry. The electromagnetic Green's function retrieval representations can be envisaged as coherent interferometric radiometry. Slob et al. [17] derived formulations for interferometry by cross correlation and by cross convolution. These rely on the block-diagonal structure of the constitutive matrix corresponding to ordinary anisotropic media. Representations have been derived for two different configurations. In the first configuration the receivers are enclosed by the sources on a closed boundary, while in the second one of the receivers is outside the closed boundary. Numerical results demonstrated that when the dissipation is weak, the results only suffer from amplitude errors, but the arrival times of the events are correct and no spurious events result from the cross correlations. Slob and Wapenaar [18] showed for the electromagnetic representations in how far field approximations lead to practical applications without the occurrence of spurious events in the results. They showed for both configurations that Green's function extraction

is possible without contributions of sources distributed in the volume when the medium only dissipates energy outside the boundary [19].

Weaver starts with Ward identities for linear acoustics in a recent acoustic derivation for Green's function retrieval by correlations of diffuse fields [20]. He suggests that Coriolis forces in mechanics and Lorentz forces in electrodynamics can be incorporated starting with Ward identities, but no proof was given. The incorporation of Coriolis forces in acoustics has been established in the Green's function retrieval formulation based on reciprocity theory [21]. In this paper the Green's function is retrieved for general linear electromagnetic media, characterized by full constitutive matrices [22] including the effects of Lorentz forces. It is shown that the principle of Green's function retrieval by cross-correlation holds for general bianisotropic materials. The constitutive matrices have symmetry properties that follow from the physics of chiral and gyrotropic media. An early example is the dual polarized ring laser [23] that can be used in downhole formation testing for oil exploration. Bianisotropic media are of growing importance in the fabrication of metamaterials [24] that can be used in transmission lines and waveguide structures [25, 26], circuits [27], absorbers [28] and in multi-band patch antennas [29]. Also macroscopically chiral media have been designed [30–36]. They extend from the microwave range to the optical regime. The theory developed here can be of interest for, passive or active, coherent interferometric radiometry in the available electromagnetic spectrum.

spectrum.

## 2. RECIPROCITY AND POWER BALANCE

The theory is developed in six-vector notation [33] and uses a unitary six-matrix, $\mathbf{K}$, as,

$$\mathbf{K} = \begin{pmatrix} -\mathbf{I} & \mathbf{O} \\ \mathbf{O} & \mathbf{I} \end{pmatrix}, \tag{1}$$

and the unit matrix $\mathbf{I}$ is used for the $3\times3$ and $6\times6$ unit matrix, but no confusion occurs. Note that $\mathbf{K}^T = \mathbf{K} = \mathbf{K}^{-1}$. The macroscopic space-time electromagnetic field is determined by the electric field $\mathbf{E}(\mathbf{x},t)$, the magnetic field $\mathbf{H}(\mathbf{x},t)$, the electric and magnetic flux densities $\mathbf{D}(\mathbf{x},t), \mathbf{B}(\mathbf{x},t)$, and the external source volume densities of electric and magnetic currents, $\{\mathbf{J}^e(\mathbf{x},t), \mathbf{J}^m(\mathbf{x},t)\}$, respectively. The time-Fourier transform of a space-time dependent quantity is defined as $\hat{f}(\boldsymbol{x},\omega) = \int \exp(-\mathrm{j}\omega t) f(\mathbf{x},t)\mathrm{d}t$, where j is the imaginary unit and $\omega$ denotes angular frequency. The frequency domain constitutive relations are given by $\hat{\mathbf{D}} = \hat{\boldsymbol{\varepsilon}}\hat{\mathbf{E}} + \hat{\boldsymbol{\xi}}\hat{\mathbf{H}}$ and $\hat{\mathbf{B}} = \hat{\boldsymbol{\zeta}}\hat{\boldsymbol{E}} + \hat{\boldsymbol{\mu}}\hat{\mathbf{H}}$ where electric

permittivity and magnetic permeability tensors are given by $\hat{\boldsymbol{\varepsilon}}$ and $\hat{\boldsymbol{\mu}}$, while $\hat{\boldsymbol{\xi}}$, $\hat{\boldsymbol{\zeta}}$ denote the magneto-electric tensors. The effects of moving media and all possible time-relaxation mechanisms are incorporated in the frequency dependent complex valued material tensors. Maxwell's equations read $\mathbf{D}_x\hat{\mathbf{u}} + \mathrm{j}\omega\hat{\mathbf{M}}\hat{\mathbf{u}} = \hat{\mathbf{s}}$, where the field vector $\hat{\mathbf{u}}$ is given by $\hat{\mathbf{u}}^T(\mathbf{x},\omega) = (\hat{\mathbf{E}}^T, \hat{\mathbf{H}}^T)$ and the superscript $T$ denotes transposition, $\hat{\mathbf{s}}^T(\mathbf{x},\omega) = -(\{\hat{\mathbf{J}}^e\}^T, \{\hat{\mathbf{J}}^m\}^T)$ is the source vector, while $\mathbf{D}_x$ is the matrix of spatial differential operators given by

$$\mathbf{D}_x = \begin{pmatrix} \mathbf{O} & \mathbf{D}_0^T \\ \mathbf{D_0} & \mathbf{O} \end{pmatrix}, \quad \mathbf{D_0} = \begin{pmatrix} 0 & -\partial_3 & \partial_2 \\ \partial_3 & 0 & -\partial_1 \\ -\partial_2 & \partial_1 & 0 \end{pmatrix}. \tag{2}$$

The material matrix is defined as

$$\hat{\mathbf{M}} = \begin{pmatrix} \hat{\boldsymbol{\varepsilon}} & \hat{\boldsymbol{\xi}} \\ \hat{\boldsymbol{\zeta}} & \hat{\boldsymbol{\mu}} \end{pmatrix}. \tag{3}$$

The following symmetry property is satisfied by the derivative matrix, $\mathbf{K}\mathbf{D}_x\mathbf{K} = -\mathbf{D}_x = -\mathbf{D}_x^T$, and it is noted that the superscript $T$ is used for matrix transposition and not for operator transposition.

A reciprocity theorem relates two states, labeled $A$ and $B$, that can be non-identical everywhere. The reciprocity theorem of the time-convolution type is used and applied to a bounded spatial domain $\mathbb{D}$, and outer boundary $\partial\mathbb{D}$ with outward pointing unit normal vector $\mathbf{n}^T = \{n_1, n_2, n_3\}$. With the above definitions, the theorem reads [34]

$$\begin{aligned} &\int_{\mathbb{D}} \left[\hat{\mathbf{u}}_A^T\mathbf{K}\hat{\mathbf{s}}_B - \hat{\mathbf{s}}_A^T\mathbf{K}\hat{\mathbf{u}}_B\right] \mathrm{d}^3\mathbf{x} \\ &= \oint_{\partial\mathbb{D}} \hat{\mathbf{u}}_A^T\mathbf{K}\mathbf{N}_x\hat{\mathbf{u}}_B \mathrm{d}^2\mathbf{x} + \mathrm{j}\omega \int_{\mathbb{D}} \left[\hat{\mathbf{u}}_A^T\left(\mathbf{K}\hat{\mathbf{M}}_B - \hat{\mathbf{M}}_A^T\mathbf{K}\right)\hat{\mathbf{u}}_B\right] \mathrm{d}^3\mathbf{x} \end{aligned} \tag{4}$$

where $\mathbf{N}_x$ is defined similar to $\mathbf{D}_x$, given by

$$\mathbf{N}_x = \begin{pmatrix} \mathbf{O} & \mathbf{N}_0^T \\ \mathbf{N}_0 & \mathbf{O} \end{pmatrix}, \quad \mathbf{N}_0 = \begin{pmatrix} 0 & -n_3 & n_2 \\ n_3 & 0 & -n_1 \\ -n_2 & n_1 & 0 \end{pmatrix}. \tag{5}$$

Equation (4) is the general representation for two independent electromagnetic states in bianisotropic media. The sources and source locations as well as the media in the two states can be completely different. The first integral in the right-hand side of Equation (4) represents the boundary integral over the outer boundary, where continuity conditions apply.

The volume integral in the right-hand side of Equation (4) vanishes when $\hat{\mathbf{M}}_A = \mathbf{K}\hat{\mathbf{M}}_B^T\mathbf{K}$, which implies that $\hat{\boldsymbol{\varepsilon}}_A = \hat{\boldsymbol{\varepsilon}}_B^T$, $\hat{\boldsymbol{\mu}}_A = \hat{\boldsymbol{\mu}}_B^T$, $\hat{\boldsymbol{\zeta}}_A = -\hat{\boldsymbol{\xi}}_B^T$ and $\hat{\boldsymbol{\xi}}_A = -\hat{\boldsymbol{\zeta}}_B^T$. The two media for which this occurs are each other's adjoint. For example an ordinary reciprocal anisotropic lossless medium becomes bianisotropic when it is moving with velocity $\mathbf{v}_A$ and the magneto-electric tensor elements are given by $\xi_{ik;A} = (\varepsilon_A\mu_A - \varepsilon_0\mu_0)\epsilon_{ijk}v_{j;A}$ and $\zeta_{mn;A} = \xi_{nm;A}$ [35]. It is clear that if $\mathbf{v}_B = -\mathbf{v}_A$ the two media are each other's adjoint and the volume integral vanishes from Equation (4). If state $A$ is a gyrotropic plasma, then the adjoint state $B$ has a DC magnetic field in the opposite direction [36] and a moving gyrotropic plasma has an adjoint medium with both the DC magnetic field and the velocity in the opposite directions [22]. The adjoint medium is denoted $\hat{\mathbf{M}}^{(a)}$ and its relation to the material matrix is given by $\hat{\mathbf{M}}^{(a)} = \mathbf{K}\hat{\mathbf{M}}^T\mathbf{K}$. In an anisotropic non-reciprocal medium the wave velocity depends on the polarization and on the direction of propagation. If these conditions hold in one and the same medium, the medium is called self-adjoint or reciprocal [37] and the material matrix satisfies $\hat{\mathbf{M}} = \mathbf{K}\hat{\mathbf{M}}^T\mathbf{K}$.

### 2.1. Source-receiver Reciprocity

The Green's function expression of source-receiver reciprocity is obtained taking state $B$ as the adjoint of state $A$, and hence the volume integral in the right-hand side of Equation (4) vanishes. The material matrices are given by $\hat{\mathbf{M}}_A = \hat{\mathbf{M}}$ and $\hat{\mathbf{M}}_B = \hat{\mathbf{M}}^{(a)}$, and the $6 \times 1$ source vectors $\hat{\mathbf{s}}_{A,B}(\mathbf{x}, \omega)$ are replaced by the $6 \times 6$ unit strength point source matrices $\mathbf{I}\delta(\mathbf{x} - \mathbf{x}_{A,B})$, where $\mathbf{I}$ is the identity matrix. The field vector $\hat{\mathbf{u}}_A(\mathbf{x}, \omega)$ is correspondingly replaced by the $6\times6$ Green's matrix $\hat{\mathbf{G}}(\mathbf{x}, \mathbf{x}_A, \omega)$, while the field vector $\hat{\mathbf{u}}_B$ is replaced by the adjoint Green's matrix $\hat{\mathbf{G}}^{(a)}(\mathbf{x}, \mathbf{x}_B, \omega)$. In the Green's matrix each column represents the Green's functions for all the electric and magnetic field components for a single source type and direction, while each row represents a single field type and component for all source types and directions. If we take $\mathbf{x}_A$ and $\mathbf{x}_B$ inside $\mathbb{D}$ and assume that outside some sphere with finite radius the medium is isotropic and homogeneous, then the boundary integral also vanishes, leaving the source-receiver reciprocity relation as

$$\mathbf{K}\hat{\mathbf{G}}^T(\mathbf{x}_B, \mathbf{x}_A, \omega)\mathbf{K} = \hat{\mathbf{G}}^{(\mathrm{a})}(\mathbf{x}_A, \mathbf{x}_B, \omega), \tag{6}$$

which expresses the equality of a measurement in a certain medium to an other measurement in its adjoint medium, with interchanged source and receiver type, vector component and location. The matrix $\mathbf{K}$ accounts for sign changes upon interchanging source and receiver.

### 2.2. Power Balance

The interferometric relation that is derived in this paper originates in the correlation-type reciprocity theorem, which reads [34],

$$\int_{\mathbb{D}} \left[\hat{\mathbf{u}}_A^{\dagger}\hat{\mathbf{s}}_B + \hat{\mathbf{s}}_A^{\dagger}\hat{\mathbf{u}}_B\right] \mathrm{d}^3\mathbf{x} = \oint_{\partial\mathbb{D}} \hat{\mathbf{u}}_A^{\dagger}\mathbf{N}_x\hat{\mathbf{u}}_B \mathrm{d}^2\mathbf{x} - \mathrm{j}\omega \int_{\mathbb{D}} \hat{\mathbf{u}}_A^{\dagger}\left(\hat{\mathbf{M}}_A^{\dagger} - \hat{\mathbf{M}}_B\right)\hat{\mathbf{u}}_B \mathrm{d}^3\mathbf{x}, \qquad (7)$$

where the superscript † denotes matrix transposition and complex conjugation. Poynting's theorem is obtained when the media and the sources in the two states are taken the same in Equation (7). From Poynting's theorem it can be deduced that for a lossless medium the volume integral in the right-hand side of Equation (7) should vanish. Hence for a lossless medium $\hat{\boldsymbol{\varepsilon}} = \hat{\boldsymbol{\varepsilon}}^{\dagger}, \hat{\boldsymbol{\mu}} = \hat{\boldsymbol{\mu}}^{\dagger}, \hat{\boldsymbol{\zeta}} = \hat{\boldsymbol{\xi}}^{\dagger}$ hold. This implies that for a lossless reciprocal medium, with $\hat{\boldsymbol{\varepsilon}} = \hat{\boldsymbol{\varepsilon}}^{T}, \hat{\boldsymbol{\mu}} = \hat{\boldsymbol{\mu}}^{T}, \hat{\boldsymbol{\zeta}} = -\hat{\boldsymbol{\xi}}^{T}$, the parameters obey $\Im\{\hat{\boldsymbol{\varepsilon}}\} = \mathbf{0}$, $\Im\{\hat{\boldsymbol{\mu}}\} = \mathbf{0}$ and $\Re\{\hat{\boldsymbol{\zeta}}\} = \mathbf{0}$ and $\Re\{\hat{\boldsymbol{\xi}}\} = \mathbf{0}$, and it is an example of a chiral medium [38]. For a lossless non-reciprocal medium we have $\Im\{\hat{\boldsymbol{\zeta}}\} = \mathbf{0}$ and $\Im\{\hat{\boldsymbol{\xi}}\} = \mathbf{0}$ and $\Re\{\hat{\boldsymbol{\zeta}}\} = \Re\{\hat{\boldsymbol{\xi}}^{T}\}$. From energy considerations it is known that lossless media have Hermitian electric permittivity and magnetic permeability, while their anti-Hermitian parts represent the wave energy dissipation [39]. From the above observations it can be deduced that for reciprocal media the frequency dependent real parts of $\hat{\boldsymbol{\varepsilon}}$ and $\hat{\boldsymbol{\mu}}$ represent reactive and inductive processes, while their imaginary parts represent resistive or absorptive processes [40]. For $\hat{\boldsymbol{\xi}}$ and $\hat{\boldsymbol{\zeta}}$ it is exactly the opposite.

### 2.3. Correlation Type Green's Matrix Representation

Equation (7) is used to derive a representation of the Green's matrix in terms of cross correlations. Point source matrices and Green's matrices are used to replace the source and field vectors. The points $\mathbf{x}_A$ and $\mathbf{x}_B$ are chosen in $\mathbb{D}$ and both states have the same medium parameters $\hat{\mathbf{M}}_A = \hat{\mathbf{M}}_B = \hat{\mathbf{M}}$. With these choices the correlation type Green's matrix representation is given by

$$\hat{\mathbf{G}}^{\dagger}(\mathbf{x}_B, \mathbf{x}_A, \omega) + \hat{\mathbf{G}}(\mathbf{x}_A, \mathbf{x}_B, \omega) = \oint_{\partial\mathbb{D}} \hat{\mathbf{G}}^{\dagger}(\mathbf{x}, \mathbf{x}_A, \omega)\mathbf{N}_x\hat{\mathbf{G}}(\mathbf{x}, \mathbf{x}_B, \omega)\mathrm{d}^2\mathbf{x} + \int_{\mathbb{D}} \hat{\mathbf{G}}^{\dagger}(\mathbf{x}, \mathbf{x}_A, \omega)\Delta\hat{\mathbf{M}}\hat{\mathbf{G}}(\mathbf{x}, \mathbf{x}_B, \omega)\mathrm{d}^3\mathbf{x}, \qquad (8)$$

where the contrast function $\hat{\mathbf{M}}$ is Hermitian and given by

$$\Delta\hat{\mathbf{M}} = \mathrm{j}\omega\left(\hat{\mathbf{M}} - \hat{\mathbf{M}}^{\dagger}\right). \tag{9}$$

It is noted that now both states exist in one and the same medium. Furthermore, these states can occur simultaneously, but that is not mandatory. No assumptions about the material matrix $\hat{\mathbf{M}}$ have been made. Only the anti-Hermitian part of $\hat{\mathbf{M}}$ remains in the representation, which was identified as the part accounting for energy dissipation. Equation (8) represents the Green's functions between $\mathbf{x}_A$ and $\mathbf{x}_B$ obtained from integral contributions of received Green's functions at the boundary $\partial\mathbb{D}$ and in the volume $\mathbb{D}$, in a general bianisotropic medium.

## 3. GREEN'S FUNCTION RETRIEVAL

Equation (8) is not suitable for Green's function retrieval, because the Green's functions under the integral are for receivers on the boundary and not at the points $\mathbf{x}_A$ and $\mathbf{x}_B$. Equation (6) could be used to interchange source and receiver positions of these Green's functions, but this would lead to Green's functions in the adjoint state. Instead, we use Equation (7) to derive an interferometric representation of the Green's matrix in terms of cross correlations. The points $\mathbf{x}_A$ and $\mathbf{x}_B$ are again chosen in $\mathbb{D}$, but the adjoint states are chosen for both $A$ and $B$, hence again both states occur in one and the same medium but now with $\hat{\mathbf{M}}_A = \hat{\mathbf{M}}_B = \hat{\mathbf{M}}^{(\mathrm{a})}$. Point source matrices are used and, as a consequence of the medium parameters, adjoint Green's matrices replace the source and field vectors. Equation (6) is used together with the symmetry relations for $\mathbf{N}_x$, and $\hat{\mathbf{M}}^{(a)}$. Transposing both sides of the resulting equation yields

$$\hat{\mathbf{G}}(\mathbf{x}_B,\mathbf{x}_A,\omega)+\hat{\mathbf{G}}^{\dagger}(\mathbf{x}_A,\mathbf{x}_B,\omega) = -\oint_{\partial\mathbb{D}} \hat{\mathbf{G}}(\mathbf{x}_B,\mathbf{x},\omega)\mathbf{N}_x\hat{\mathbf{G}}^{\dagger}(\mathbf{x}_A,\mathbf{x},\omega)\mathrm{d}^2\mathbf{x} + \int_{\mathbb{D}} \hat{\mathbf{G}}(\mathbf{x}_B,\mathbf{x},\omega)\Delta\hat{\mathbf{M}}\hat{\mathbf{G}}^{\dagger}(\mathbf{x}_A,\mathbf{x},\omega)\mathrm{d}^3\mathbf{x}, \tag{10}$$

where the contrast function $\Delta\hat{\mathbf{M}}$ is the same as in Equation (9). No assumptions about the material matrix $\hat{\mathbf{M}}$ has been made, other than that its adjoint exists.

Equation (10) is a general representation of the electromagnetic Green's matrix, between $\mathbf{x}_A$ and $\mathbf{x}_B$ located in the same medium. It is obtained from integral contributions of cross correlations of field

recordings from sources at the boundary, $\partial\mathbb{D}$ and inside the volume, $\mathbb{D}$, in an arbitrary heterogeneous bianisotropic medium. It is valid for reciprocal and non-reciprocal media. When the medium dissipates no energy, the full Green's matrix can be obtained from sources on the boundary only. Hence, even for an arbitrary bianisotropic medium, absence of energy dissipation is a sufficient condition for obtaining the Green's function from the cross correlation of two recordings, at $\mathbf{x}_A$ and $\mathbf{x}_B$, from sources on a boundary only.

In the time domain the Green's matrix is causal, hence $\mathbf{G}(\mathbf{x}_B, \mathbf{x}_A, t) = \mathbf{0}$ for $t < 0$, and the time reversed Green's function is time reversed causal, hence $\mathbf{G}^T(\mathbf{x}_A, \mathbf{x}_B, -t) = \mathbf{0}$ for $t > 0$. For this reason $\mathbf{G}(\mathbf{x}_B, \mathbf{x}_A, t)$ or $\mathbf{G}^T(\mathbf{x}_A, \mathbf{x}_B, -t)$ can be easily retrieved from the left-hand side of Equation (10), $\mathbf{G}(\mathbf{x}_B, \mathbf{x}_A, t) + \mathbf{G}^T(\mathbf{x}_A, \mathbf{x}_B, -t)$, by taking the causal or time-reversed causal part, respectively. In general, the application of Equation (10) requires independent measurements of sources at all points in the domain and at the boundary of $\mathbb{D}$. Apart from the usefulness of this relation for modeling and inversion [41, 42], and for validation of numerical codes, here the primary interest is in possible applications of remote sensing without a source.

Two types of symmetry are distinguished for the magneto-electric tensors, i.e., $\hat{\boldsymbol{\zeta}} = \hat{\boldsymbol{\xi}}^T$ for non-reciprocal media and $\hat{\boldsymbol{\zeta}} = -\hat{\boldsymbol{\xi}}^T$ for reciprocal media. To facilitate the further development the magneto-electric parameter tensors are split in their real and imaginary parts and two new real-valued tensors are introduced, $\hat{\boldsymbol{\chi}}$ and $\hat{\boldsymbol{\kappa}}$, such that $\hat{\boldsymbol{\xi}} = \hat{\boldsymbol{\chi}} + \mathrm{j}\hat{\boldsymbol{\kappa}}$ and $\hat{\boldsymbol{\zeta}} = \hat{\boldsymbol{\chi}} - \mathrm{j}\hat{\boldsymbol{\kappa}}$. For a reciprocal medium $\hat{\mathbf{M}} = \mathbf{K}\hat{\mathbf{M}}^T\mathbf{K}$ implying that $\hat{\boldsymbol{\varepsilon}} = \hat{\boldsymbol{\varepsilon}}^T$, $\hat{\boldsymbol{\mu}} = \hat{\boldsymbol{\mu}}^T$, $\hat{\boldsymbol{\chi}} = -\hat{\boldsymbol{\chi}}^T$ and $\hat{\boldsymbol{\kappa}} = \hat{\boldsymbol{\kappa}}^T$. It is lossless when $\Im\{\hat{\boldsymbol{\varepsilon}}\} = \mathbf{0}$, $\Im\{\hat{\boldsymbol{\mu}}\} = \mathbf{0}$ and $\hat{\boldsymbol{\chi}} = \mathbf{0}$. Optical activity or left- and right-handedness in general fall under this category and media with such properties are also engineered to make negative refractive index materials [27]. A non-reciprocal medium is characterized by $\hat{\boldsymbol{\chi}} = \hat{\boldsymbol{\chi}}^T$ and $\hat{\boldsymbol{\kappa}} = -\hat{\boldsymbol{\kappa}}^T$. A moving medium falls in the category of non-reciprocal media. The permittivity and permeability tensors can be defined by off-diagonal elements that have equal magnitude but opposite signs, $\hat{\boldsymbol{\varepsilon}} - \mathrm{diag}(\hat{\boldsymbol{\varepsilon}}) = \mathrm{diag}(\hat{\boldsymbol{\varepsilon}}) - \hat{\boldsymbol{\varepsilon}}^T$ and $\hat{\boldsymbol{\mu}} - \mathrm{diag}(\hat{\boldsymbol{\mu}}) = \mathrm{diag}(\hat{\boldsymbol{\mu}}) - \hat{\boldsymbol{\mu}}^T$. Engineered materials in this class are also studied for possible negative refractive indices [43].

The major difference between non-reciprocal and reciprocal media is the accumulation of polarization rotation in non-reciprocal media upon multiple back and forth passages through such a medium, while the average polarization rotation is zero in multiple back and forth passages through a reciprocal medium [44]. Finally, it is easy to combine both classes in a so-called *lossless gyrotropic chiral* medium. This is a general concept because such models allow our the

representations to be used for moving media and Lorenz forces, electric and magnetic birefringence, Fresnel-Fizeau effects, optical activity and both electric and magnetic Faraday rotations [45]. Here the lossless variant is of interest with $\hat{\mathbf{M}} = \hat{\mathbf{M}}^\dagger$, where dispersion can occur but no energy is dissipated. For the situation of strongly dissipative media and with sources on a plane boundary only, a method was developed based on a deconvolution technique that retrieves the reflection response for elastic and diffusive electromagnetic fields [46] and applied to ground-penetrating radar [47].

### 3.1. Lossless Gyrotropic Chiral Media

General bianisotropic lossless media are defined by taking Hermitian matrices for the medium parameters, $\hat{\mathbf{M}} = \hat{\mathbf{M}}^\dagger$ leading to $\Delta\hat{\mathbf{M}} = \mathbf{0}$. Note that this form allows the electric permittivity and magnetic permeability tensors to be Hermitian tensors, $\hat{\boldsymbol{\varepsilon}} = \hat{\boldsymbol{\varepsilon}}^\dagger$ and $\hat{\boldsymbol{\mu}} = \hat{\boldsymbol{\mu}}^\dagger$, allowing for describing dispersive non-dissipative processes, while $\hat{\boldsymbol{\chi}}$ and $\hat{\boldsymbol{\kappa}}$ are symmetric tensors. With these symmetry conditions of the material matrices, Equation (10) directly reduces to,

$$\hat{\mathbf{G}}(\mathbf{x}_B, \mathbf{x}_A, \omega) + \hat{\mathbf{G}}^\dagger(\mathbf{x}_A, \mathbf{x}_B, \omega) = -\oint_{\partial\mathbb{D}} \hat{\mathbf{G}}(\mathbf{x}_B, \mathbf{x}, \omega)\mathbf{N}_x\hat{\mathbf{G}}^\dagger(\mathbf{x}_A, \mathbf{x}, \omega)\mathrm{d}^2\mathbf{x}. \tag{11}$$

For lossless media the Green's matrix between $\mathbf{x}_A$ and $\mathbf{x}_B$ is obtained from cross correlations of recordings from responses to independent impulsive sources on $\partial\mathbb{D}$ only. This representation is valid for non-reciprocal and reciprocal lossless media. To make Equation (11) suited for uncorrelated noise sources, $\mathbf{N}_x$ must be diagonalized. This involves the separation of contributions from the sources for inward and outward traveling waves. This is achieved by a bi-directional modal decomposition as outlined in [16]. It is possible when the medium outside the boundary is homogeneous and the boundary itself is in the far field of the receivers. Then it leads to an asymptotically exact result in case the boundary containing the noise sources is in the far field of the medium for which one would like to find the Green's function. An example of the diagonalization procedure is given in [17] for an isotropic medium outside $\mathbb{D}$. Then, e.g., the electric subset of Equation (11) is in the time domain given by,

$$\begin{aligned}&\left\{\mathbf{G}^{Ee}(\mathbf{x}_B, \mathbf{x}_A, t) + \left[\mathbf{G}^{Ee}(\mathbf{x}_A, \mathbf{x}_B, -t)\right]^T\right\}\\ &\propto \oint_{\partial\mathbb{D}} \mathbf{G}^{Ee}(\mathbf{x}_B, \mathbf{x}, t) * [\mathbf{G}^{Ee}(\mathbf{x}_A, \mathbf{x}, -t)]^T \mathrm{d}^2\mathbf{x},\end{aligned} \tag{12}$$

where time convolution is indicated by $*$, the Green's function corresponding to the electric field due to an electric current source is represented by $\mathbf{G}^{Ee}$. If uncorrelated noise sources are present on the boundary such that the observed electric field vector can be written as

$$\mathbf{E}^{\mathrm{obs}}(\mathbf{x}_A,t)=\oint_{\mathbf{x}\in\partial\mathbb{D}}\mathbf{G}(\mathbf{x}_A,\mathbf{x},t)*\mathbf{S}(\mathbf{x},t)\mathrm{d}^2\mathbf{x}, \tag{13}$$

$$\mathbf{E}^{\mathrm{obs}}(\mathbf{x}_B,t)=\oint_{\mathbf{x}'\in\partial\mathbb{D}}\mathbf{G}(\mathbf{x}_B,\mathbf{x}',t)*\mathbf{S}(\mathbf{x}',t)\mathrm{d}^2\mathbf{x}', \tag{14}$$

such that

$$\mathbf{S}(\mathbf{x},t)*\mathbf{S}(\mathbf{x}',-t)=C(t)\delta(\mathbf{x}-\mathbf{x}')\mathbf{I}, \tag{15}$$

where $C(t)$ denotes the autocorrelation of the noise sources.

$$\begin{aligned}&\left\{\mathbf{G}^{Ee}(\mathbf{x}_B,\mathbf{x}_A,t)+\left[\mathbf{G}^{Ee}(\mathbf{x}_A,\mathbf{x}_B,-t)\right]^T\right\}*C(t)\\&\propto\mathbf{E}^{\mathrm{obs}}(\mathbf{x}_B,t)*\left\{\mathbf{E}^{\mathrm{obs}}(\mathbf{x}_A,-t)\right\}^T.\end{aligned} \tag{16}$$

For random white noise sources the autocorrelation function is given by $C(t)=\delta(t)$, and the Green's function is retrieved.

### 3.2. Two Dimensional Example

To illustrate the concept a two-dimensional TE-mode example is given in detail. The configuration consists of a lossless bianisotropic medium, characterized by the following constitutive relations

$$\hat{D}_2(x_1,x_3\omega)=\varepsilon\hat{E}_2(x_1,x_3,\omega)+\xi_{21}\hat{H}_1(x_1,x_3,\omega)+\xi_{23}\hat{H}_3(x_1,x_3,\omega), \tag{17}$$

$$\hat{B}_1(x_1,x_3,\omega)=\zeta_{12}\hat{E}_2(x_1,x_3,\omega)+\mu\hat{H}_1(x_1,x_3,\omega), \tag{18}$$

$$\hat{B}_3(x_1,x_3,\omega)=\zeta_{32}\hat{E}_2(x_1,x_3,\omega)+\mu\hat{H}_3(x_1,x_3,\omega), \tag{19}$$

with real valued position dependent functions $\varepsilon(x_1,x_3)$ and $\mu(x_1,x_3)$ and the condition that $\xi_{kr}(x_1,x_3)=\zeta^*_{rk}(x_1,x_3)$. The reciprocity theorem of the time-correlation type is used in a bounded two-dimensional domain $\mathbb{S}$, with outward unit normal $\mathbf{n}=(n_1,0,n_3)^T$, in a medium that is adjoint to the medium for which the Green's function is retrieved. Hence by choosing both states, as before, with equal medium parameters we have $\Delta\hat{\mathbf{M}}=\mathbf{0}$. The field equations for

the adjoint medium are given by

$$\begin{pmatrix} 0 & -\partial_3 & \partial_1 \\ -\partial_3 & 0 & 0 \\ \partial_1 & 0 & 0 \end{pmatrix} \begin{pmatrix} \hat{E}_2^{(\mathrm{a})} \\ \hat{H}_1^{(\mathrm{a})} \\ \hat{H}_3^{(\mathrm{a})} \end{pmatrix} - \mathrm{j}\omega \begin{pmatrix} -\varepsilon & \zeta_{12} & \zeta_{32} \\ \xi_{21} & -\mu & 0 \\ \xi_{23} & 0 & -\mu \end{pmatrix} \begin{pmatrix} \hat{E}_2^{(\mathrm{a})} \\ \hat{H}_1^{(\mathrm{a})} \\ \hat{H}_3^{(\mathrm{a})} \end{pmatrix} = \begin{pmatrix} -\hat{J}_2^e \\ 0 \\ 0 \end{pmatrix}, \tag{20}$$

where the superscript (a) denotes the field in the adjoint medium, and the explicit expressions for the adjoint medium parameters in terms of the actual medium parameters have been used. The reciprocity theorem of the time correlation type of Equation (7) reduces to

$$\begin{aligned} &\int_{\mathbb{S}} \left[ \left\{ \hat{E}_{2;A}^{(\mathrm{a})} \right\}^* \hat{J}_{2;B}^e + \hat{E}_{2;B}^{(\mathrm{a})} \left\{ \hat{J}_{2;A}^e \right\}^* \right] \mathrm{d}^2\mathbf{x} \\ &= \frac{1}{\mathrm{j}\omega} \oint_{\partial\mathbb{S}} \mu^{-1} \left[ \left\{ \hat{E}_{2;A}^{(\mathrm{a})} \right\}^* n_m \partial_m \hat{E}_{2;B}^{(\mathrm{a})} - \hat{E}_{2;B}^{(\mathrm{a})} n_m \partial_m \left\{ \hat{E}_{2;A}^{(\mathrm{a})} \right\}^* \right] \mathrm{d}\mathbf{x} \\ &+ 2 \oint_{\partial\mathbb{S}} \mu^{-1} \epsilon_{km2} n_k \Re\{\xi_{2m}\} \left\{ \hat{E}_{2;A}^{(\mathrm{a})} \right\}^* \hat{E}_{2;B}^{(\mathrm{a})} \mathrm{d}\mathbf{x}, \end{aligned} \tag{21}$$

where it is understood that $n_2 = 0$ in this two-dimensional example. The second and third equations from (20) have been used to write the magnetic field in terms of the electric field, which is the diagonalization procedure, mentioned above. As a consequence of this, it can be seen in Equation (21) that for a lossless non-reciprocal medium, where $\xi_{kr}$ has a non-vanishing real part, an extra integral over the boundary remains in the time-correlation type reciprocity theorem compared to an ordinary anisotropic and reciprocal lossless medium. For a bianisotropic reciprocal lossless medium $\Re\{\xi_{kr}\} = 0$ and hence the second integral in the right-hand side of Equation (21) vanishes. In that case Equation (21) reduces to the same form as for an ordinary anisotropic reciprocal lossless medium.

The next step is to assume that the medium in the neighborhood of the boundary $\partial\mathbb{S}$ is homogeneous. In the high-frequency approximation the normal derivative of the electric field can be approximated as $n_m \partial_m \hat{E}_2^{(\mathrm{a})}(\mathbf{x}, \omega) \approx -\mathrm{j}\omega \hat{E}_2^{(\mathrm{a})}(\mathbf{x}, \omega)/c$, where $c$ is the electromagnetic wave propagation velocity in an ordinary isotropic medium, which approximation assumes a normally outward propagating wave and the bianisotropy parameters are assumed to be much smaller than $1/c$, hence $\xi_{2r}\zeta_{r2} \ll \varepsilon\mu$. The small bianisotropy parameter assumption

leads to a negligible contribution of the second integral in the right-hand side of Equation (21) compared to the contribution from the first integral. Applying the high frequency approximation and the small bianisotropy parameter assumption to Equation (21), results in

$$\int_{\mathbb{S}}\Big[\Big\{\hat{E}^{(\mathrm{a})}_{2;A}\Big\}^{*}\hat{J}^{e}_{2;B}+\hat{E}^{(\mathrm{a})}_{2;B}\Big\{\hat{J}^{e}_{2;A}\Big\}^{*}\Big]\,\mathrm{d}^2\mathbf{x}\approx-\frac{2}{\mu c}\oint_{\partial\mathbb{S}}\Big\{\hat{E}^{(\mathrm{a})}_{2;A}\Big\}^{*}\hat{E}^{(\mathrm{a})}_{2;B}\mathrm{d}\mathbf{x}. \quad (22)$$

Now choices can be made for the sources in state $A$ as $\hat{J}^{e}_{2;A} = \delta(x_1-x_{1;A})\delta(x_3-x_{3;A})$ and in state $B$ as $\hat{J}^{e}_{2;B} = \delta(x_1-x_{1;B})\delta(x_3-x_{3;B})$. The corresponding two-dimensional electric field Green's function of the adjoint medium due to an electric current source is introduced as $\hat{G}^{(\mathrm{a})}(\mathbf{x},\mathbf{x}',\omega)$ satisfying the wave equation given by

$$\begin{aligned}&\left[\frac{\partial_1\mu^{-1}\partial_1+\partial_3\mu^{-1}\partial_3}{\mathrm{j}\omega}+\epsilon_{2mp}\partial_m\frac{\zeta_{p2}}{\mu}-\frac{\xi_{2j}}{\mu}\epsilon_{jm2}\partial_m\right.\\&\left.+\mathrm{j}\omega\left(\frac{\xi_{2q}\zeta_{q2}}{\mu}-\varepsilon\right)\right]\hat{G}^{(\mathrm{a})}(\mathbf{x},\mathbf{x}',\omega)=\delta(\mathbf{x}-\mathbf{x}'). \quad (23)\end{aligned}$$

The electric field can be written in terms of the Green's function as $\hat{E}^{(\mathrm{a})}(\mathbf{x},\omega)=\hat{G}^{(\mathrm{a})}(\mathbf{x},\mathbf{x}',\omega)$ and is substituted in Equation (22) to obtain

$$\begin{aligned}&\Big\{\hat{G}^{(\mathrm{a})}(\mathbf{x}_B,\mathbf{x}_A,\omega)\Big\}^{*}+\hat{G}^{(\mathrm{a})}(\mathbf{x}_A,\mathbf{x}_B,\omega)\\&\approx-\frac{2}{\mu c}\oint_{\partial\mathbb{S}}\Big\{\hat{G}^{(\mathrm{a})}(\mathbf{x},\mathbf{x}_A,\omega)\Big\}^{*}\hat{G}^{(\mathrm{a})}(\mathbf{x},\mathbf{x}_B,\omega)\mathrm{d}\mathbf{x}. \quad (24)\end{aligned}$$

Exploiting the fact that $\hat{G}^{(\mathrm{a})}(\mathbf{x}',\mathbf{x},\omega)=\hat{G}(\mathbf{x},\mathbf{x}',\omega)$ all the Green's functions in Equation (24) belonging to the adjoint medium are replaced with the Green's function in the actual medium and Equation (24) is rewritten as

$$\hat{G}^{*}(\mathbf{x}_A,\mathbf{x}_B,\omega)+\hat{G}(\mathbf{x}_B,\mathbf{x}_A,\omega)\approx-\frac{2}{\mu c}\oint_{\partial\mathbb{S}}\hat{G}^{*}(\mathbf{x}_A,\mathbf{x},\omega)\hat{G}(\mathbf{x}_B,\mathbf{x},\omega)\mathrm{d}\mathbf{x}, \quad (25)$$

which is the desired Green's function retrieval equation of the Green's function between $\mathbf{x}_A$ and $\mathbf{x}_B$ from the product of the complex conjugate of the Green's function between a receiver in $\mathbf{x}_A$ and sources on the boundary $\partial\mathbb{S}$ and the Green's function between a receiver in $\mathbf{x}_B$ and sources on the boundary $\partial\mathbb{S}$. If the sources on $\partial\mathbb{S}$ are uncorrelated noise sources such that the observed electric fields can be written analogous to Equations (13) and (14), Equation (25) can be written in the time

domain as

$$\{G(\mathbf{x}_B, \mathbf{x}_A, t) + G(\mathbf{x}_A, \mathbf{x}_B, -t)\} * C(t) \approx -\frac{2}{\mu c} E_2^{\text{obs}}(\mathbf{x}_B, t) * E_2^{\text{obs}}(\mathbf{x}_A, -t), \tag{26}$$

which is the two-dimensional scalar equivalent of the general three-dimensional matrix relation of Equation (16) and with a proportionality factor of $-2/(\mu c)$. According to this equation, the cross correlation of the observed electric fields at locations $\mathbf{x}_A$ and $\mathbf{x}_B$ in a bianisotropic lossless medium, non-reciprocal or reciprocal, yields the superposition of the medium response from a source in $\mathbf{x}_A$ to the receiver in $\mathbf{x}_B$ and the time reversed response from a source in $\mathbf{x}_B$ to the receiver in $\mathbf{x}_A$, both convolved with the autocorrelation of the noise sources. Equation (26) is used in the numerical example.

### 3.3. Numerical Example

For the numerical experiment a homogeneous non-reciprocal lossless medium is taken with real constants $\varepsilon = 4\varepsilon_0$ and $\mu = \mu_0$, where $\varepsilon_0$ and $\mu_0$ denote the free space parameters. Equal real magneto-electric constants used, $\xi_{21} = \zeta_{12} = 5 \times 10^{-10}$ s/m and $\xi_{23} = \zeta_{32} = 0$. The domain $\mathbb{S}$ has a circular boundary $\partial\mathbb{S}$ with a radius of 50 cm, where the 360 noise sources are located. The noise signals are filtered around a center frequency of 10 GHz. We consider two locations $\mathbf{x}_A$ and $\mathbf{x}_B$ separated by 20 cm, each registering 24 µs of noise. Initially, the two

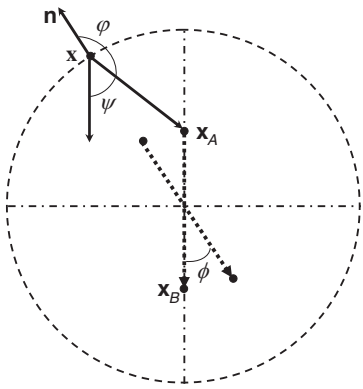


**Figure 1.** The configuration for the numerical experiment in a homogeneous bianisotropic medium with a magneto-electric coupling coecient linking the vertical magnetic field component to the TE-mode electric field component.

receivers are located on a line along the direction of bianisotropy, see Fig. 1, which is taken as the line where $\phi = 0$, being the line along the $x_3$-axis. The first 4 ns of the noise fields recorded at the locations $\mathbf{x}_A$ and $\mathbf{x}_B$ are shown in Figs. 2(a) and 2(b), respectively.

The cross correlation of the full measurement of 24 μs of these recordings is represented by the right-hand side of Equation (26). The first ±2.5 ns of the result are shown in Fig. 3(b), where the first trace represents the correlation result for $\phi = 0$. The arrival time difference for the wave field traveling from $\mathbf{x}_A$ and $\mathbf{x}_B$ and the wave field traveling from $\mathbf{x}_B$ and $\mathbf{x}_A$ is at its maximum. The wave velocity in the $+x_3$-direction (wave traveling from $\mathbf{x}_A$ to $\mathbf{x}_B$) is 13.99 cm/ns and it corresponds to the causal Green's function with an arrival time of 1.43 ns, while the wave field traveling in the $-x_3$-direction has a propagating velocity of 16.26 cm/ns and the arrival time is 1.23 ns and maps to the negative arrival time of the corresponding time-reversed Green's function. At 90° the wave velocity in the $\pm x_1$-direction is 15.04 cm/ns and the arrival time is ±1.33 ns, respectively. The other traces represent results for repeated experiments with rotated locations for $\mathbf{x}_A$ and $\mathbf{x}_B$ as indicated in Fig. 1.

By comparing the exact result of the left-hand side of Equation (26) in Fig. 3(a) and the retrieved result from cross correlations of noise recordings of the right-hand side of Equation (26) in Fig. 3(b), it can be observed that the travel times are accurately retrieved, but small errors are made in the wave field amplitude as shown in Fig. 4. These errors can be understood from the two approximations. In the approximation of the amplitude factor for the first integral in the right-hand side of Equation (21), an angle

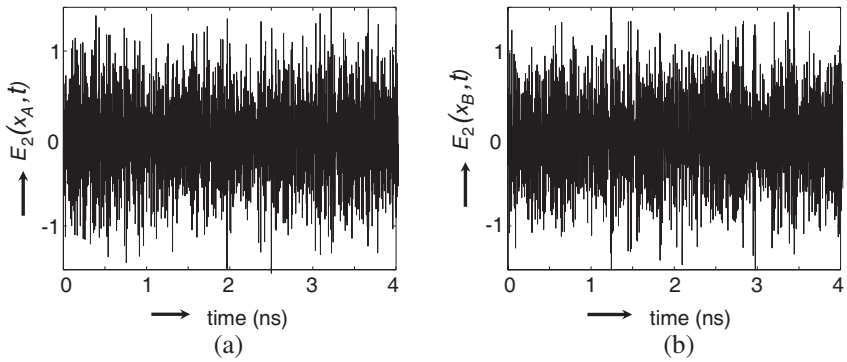


**Figure 2.** The first 4 ns of noise at the two receiver locations, $E_2(\mathbf{x}_A, t)$ (a), and $E_2(\mathbf{x}_B, t)$ (b).

independent relation was used for the normal derivative, while it is depending on the angles $\varphi$ and $\psi$, see Fig. 1. Secondly, the second integral has been neglected because of the small bianisotropy parameter assumption. The total amplitude dependence is given by $\cos(\psi)\Re(\xi_{21}) + \cos(\varphi)\sqrt{\varepsilon\mu - \xi_{21}\zeta_{12}}$, where $\psi$ is the angle between the $x_3$-direction and the line from the noise source to the receiver location,

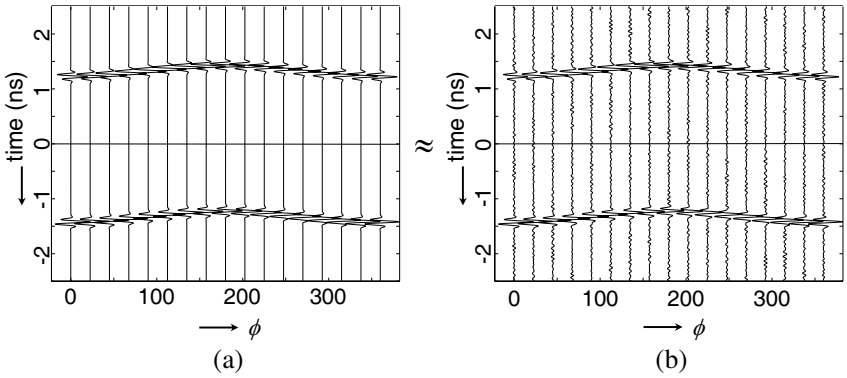


**Figure 3.** (a) The first $\pm 2.5$ ns of the left-hand side of Equation (26) and (b) the correlation result corresponding to the right-hand side of Equation (26). Both graphs show the result in the time domain as a function of the angle between the $x_3$-axis and the line containing the two receivers.

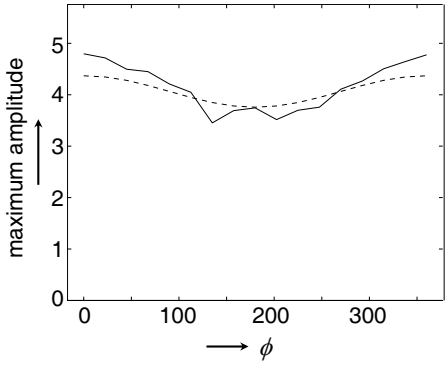


**Figure 4.** Maximum amplitude comparison between the exact solution (dashed line) of the left-hand side of Equation (26) and the retrieved result from cross correlations of the noise recordings (solid line) in the right-hand side of Equation (26) as a function of angle between the $x_3$-axis and the line containing the two receivers.

while $\varphi$ is the angle between the normal vector and the line from the noise source to the receiver, see Fig. 1. The approximation used is $\cos(\psi)\Re(\xi_{21}) + \cos(\varphi)\sqrt{\varepsilon\mu - \xi_{21}\zeta_{12}} \approx -\sqrt{\varepsilon\mu}$, which is the result obtained by taking $\cos(\psi) = 0$ and $\varepsilon\mu \gg \xi_{21}\zeta_{12}$. This means that the largest errors will occur when the points $\mathbf{x}_A$ and $\mathbf{x}_B$ are aligned along the $x_3$-axis, in which case $\psi = 0$ and $\phi = 0$, or $\psi = \pi$ and $\phi = \pi$, and the stationary points are for $\varphi = \pi$. The expected amplitude errors are therefor primarily related to the dependence on $\psi$ of the contributions from the sources on the boundary. This is approximately what can be seen in Fig. 4; maximum errors for $\phi = 0$ and $\phi = \pi$ and minimum errors for $\phi = \pi/2$ and $\phi = 3\pi/2$. The observed irregularities in the reconstructed amplitudes are due to the noise behavior of the sources.

## 4. CONCLUDING REMARKS

The representations derived here for matrix Green's function retrieval in general bianisotropic media holds for non-reciprocal and dissipative media. It applies to natural and engineered media such as gyrotropic and chiral media, including metamaterials. The symmetry properties of the material parameter tensors are given for both reciprocal and non-reciprocal lossless media. It was shown that with these symmetry properties the Green's function is retrieved by correlating measured data at two locations due to sources on a boundary only.

Not all source locations are equally important and practical configurations with open boundaries may result in accurate results, because the main contributions come from sources located at stationary points [9]. The presence of weak losses has no effects on the phase of the extracted Green's function, while some amplitude errors but no spurious events occur [17].

They may be useful in a wide variety of fields, ranging from microwave to optical regimes, and the most interesting application would be to obtain pulse-echo data from cross correlations of noise observations for imaging and characterization of natural and engineered materials [48].

## ACKNOWLEDGMENT

This work is part of the research program of the Netherlands research center for Integrated Solid Earth Science (ISES).

## REFERENCES


1. Scherbaum, F., "Seismic imaging of the site response using microearthquake recordings: Part I. Method," *Bull. Seism. Soc. Am.*, Vol. 77, No. 6, 1905–1923, 1987.
2. Scherbaum, F., "Seismic imaging of the site response using microearthquake recordings: Part I. Application to the Swabian Jura, southwest Germany, seismic network," *Bull. Seism. Soc. Am.*, Vol. 77, No. 6, 1924–1944, 1987.
3. Buckingham, M. J., B. V. Berkhout, and S. A. L. Glegg, "Imaging the ocean with ambient noise," *Nature (London)*, Vol. 356, No. 6367, 327–329, March 1992.
4. Weaver, R. and O. Lobkis, "Ultrasonics without a source: Thermal fluctuation correlations at MHz frequencies," *Phys. Rev. Lett.*, Vol. 87, No. 13, 134301-1–134301-4, 2001.
5. Campillo, M. and A. Paul, "Long-range correlations in the diffuse seismic coda waves," *Science*, Vol. 299, No. 5606, 547–549, 2003.
6. Shapiro, N., M. Campillo, L. Stehly, and M. Ritzwoller, "High-resolution surface-wave tomography from ambient seismic noise," *Science*, Vol. 307, No. 5715, 1615–1618, 2005.
7. Draganov, D., K. Wapenaar, W. Mulder, J. Singer, and A. Verdel, "Retrieval of reflections from seismic background-noise measurements," *Geoph. Res. Lett.*, Vol. 34, No. 4, L04305, 2007.
8. Schuster, G., J. Yu, J. Sheng, and J. Rickett, "Interferometric/daylight seismic imaging," *Geoph. J. Int.*, Vol. 157, No. 2, 838–852, 2004.
9. Snieder, R., "Extracting the Green's function from the correlation of coda waves: A derivation based on stationary phase," *Phys. Rev. E*, Vol. 69, No. 4, 046610-1–046610-8, 2004.
10. Wapenaar, K., "Retrieving the elastodynamic Green's function of an arbitrary inhomogeneous medium by cross correlation," *Phys. Rev. Lett.*, Vol. 93, No. 25, 254301-1–254301-4, 2004.
11. Lerosey, G., J. De Rosny, A. Tourin, A. Derode, G. Montaldo, and M. Fink, "Time reversal of electromagnetic waves," *Phys. Rev. Lett.*, Vol. 92, No. 19, 193904-1–193904–3, 2004.
12. Corbella, I., N. Duffo, M. Vall-llossera, A. Camps, and F. Torres, "The visibility function in interferometric aperture synthesis radiometry," *IEEE Trans. on Geoscience and Remote Sensing*, Vol. 42, No. 8, 1677–1682, 2004.
13. Oestges, C., A. Kim, G. Papanicolaou, and A. Paulraj, "Characterization of space-time focusing in time-reversed random

fields," *IEEE Trans. Ant. and Prop.*, Vol. 53, No. 1, 283–293, 2005.

14. Snieder, R., "Retrieving the Green's function of the diffusion equation from the response to a random forcing," *Phys. Rev. E*, Vol. 74, No. 4, 046620-1–046620-9, 2006.
15. Slob, E., D. Draganov, and K. Wapenaar, "GPR without a source," *Proceedings of the 11th International Conf. on GPR*, ANT. 6, Ohio State University, Columbus, Ohio, 2006.
16. Wapenaar, K., E. Slob, and R. Snieder, "Unified Green's function retrieval by cross correlation," *Phys. Rev. Lett.*, Vol. 97, No. 23, 234301-1–234301-4, 2006.
17. Slob, E., D. Draganov, and K. Wapenaar, "Interferometric electromagnetic Green's functions representations using propagation invariants," *Geoph. J. Int.*, Vol. 169, No. 1, 60–80, 2007.
18. Slob, E. and K. Wapenaar, "GPR without a source: Cross-correlation and cross-convolution methods," *IEEE Trans. Geoscience and Remote Sensing*, Vol. 45, No. 8, 2501–2510, 2007.
19. Slob, E. and K. Wapenaar, "Electromagnetic Green's functions retrieval by cross-correlation and cross-convolution in media with losses," *Geoph. Res. Lett.*, Vol. 34, No. 5, L05307, 2007.
20. Weaver, R., "Ward identities and the retrieval of Green's functions in the correlations of a diffuse field," *Wave Motion*, Vol. 45, No. 5, 596–604, 2008.
21. Ruigrok, E., D. Draganov, and K. Wapenaar, "Global-scale seismic interferometry: Theory and numerical examples," *Geophysical Prospecting*, Vol. 56, No. 3, 395–417, May 2008.
22. Kong, J., "Theorems of bianisotropic media," *Proceedings of the IEEE*, Vol. 60, No. 9, 1036–1046, 1972.
23. Chow, W. W., J. G.-Banacloche, L. M. Pedrotti, V. E. Sanders, W. Schleich, and M. O. Scully, "The ring laser gyro," *Rev. Mod. Phys.*, Vol. 57, No. 1, 61–104, January 1985.
24. Sihvola, A., "Metamaterials in electromagnetics," *Metamaterials*, Vol. 1, No. 1, 2–11, 2007.
25. Caloz, C. and T. Itoh, *Electromagnetic Metamaterials*, John Wiley & Sons, Inc., Hoboken, New Jersey, 2006.
26. Pitarch, J., J. M. C.-Civera, F. L. P.-Foix, and M. A. Solano, "Efficient modal analysis of bianisotropic waveguides by the coupled mode method," *IEEE Trans. on Microwave Theory and Techniques*, Vol. 55, No. 1, 108–116, 2007.
27. Cui, T.-J., H.-F. Ma, R. P. Liu, B. Zhao, Q. Cheng, and J. Y. Chin, "A symmetrical circuit model describing all kinds of

circuit metamaterials," *Progress In Electromagnetics Research B*, Vol. 5, 63–76, 2008.

28. Huang, R., Z.-W. Li, L. B. Kong, L. Liu, and S. Matitsine, "Analysis and design of an ultra-thin metamaterial absorber," *Progress In Electromagnetics Research B*, Vol. 14, 407–429, 2009.
29. Weng, Z.-B., Y.-C. Jiao, F.-S. Zhang, Y. Song, and G. Zhao, "A multi-band patch antenna on metamaterial substrate," *J. of Electromagn. Waves and Appl.*, Vol. 22, No. 2/3, 445–452, 2008.
30. Wongkasem, N., A. Akyurtlu, K. A. Marx, Q. Dong, J. Li, and W. D. Goodhue, "Development of chiral negative refractive index metamaterials for the terahertz frequency regime," *IEEE Trans. Antennas and Propagation*, Vol. 55, No. 11, 3052–3062, 2007.
31. Meiners, C. and A. F. Jacob, "Numerical and experimental parameter study of helix layers," *Trans. Antennas and Propagation*, Vol. 56, No. 5, 1321–1328, 2008.
32. Silveirinha, M. G., "Design of linear-to-circular polarization transformers made of long densely packed metallic helices," *IEEE Trans. Antennas and Propagation*, Vol. 56, No. 2, 390–401, 2008.
33. Santagata, N. M., P. Luo, A. M. Lakhani, D. J. De Witt, B. S. Day, M. L. Norton, and T. P. Pearl, "Organizational structure and electronic decoupling of surface bound chiral domains and biomolecules," *IEEE Sensors Journal*, Vol. 8, No. 6, 758–766, 2008.
34. Tajitsu, Y., "Piezoelectricity of chiral polymeric fiber and its application in biomedical engineering," *IEEE Trans. on Ultrasonics, Ferroelectrics and Frequency Control*, Vol. 55, No. 5, 1000–1008, 2008.
35. Yang, X. M., J. Y. Chin, Q. Cheng, X. Q. Lin, and T. J. Cui, "Realization and experimental verification of chiral cascaded circuit," *IEEE Microwave and Wireless Components Letters*, Vol. 18, No. 5, 308–310, 2008.
36. Dong, J. and C. Xu, "Characteristics of guided modes in planar chiral nihility meta-material waveguides," *Progress In Electromagnetics Research B*, Vol. 14, 107–126, 2009.
37. Lindell, I., A. Sihvola, and K. Suchy, "Six-vector formalism in electromagnetics of bi-anisotropic media," *Journal of Electromagnetic Waves and Applications*, Vol. 9, No. 7–8, 887–903, 1995.
38. Wapenaar, K. and J. Fokkema, "Reciprocity theorems for diffusion, flow and waves," *A.S.M.E. Journal of Applied Mechanics*, Vol. 71, No. 1, 145–150, 2004.
39. Tai, C., "A study of electrodynamics of moving media,"

*Proceedings of the IEEE*, Vol. 52, No. 6, 685–689, 1964.

40. Harrington, R. and A. Villeneuve, "Reciprocity relationships for gyrotropic media," *IRE Trans. on Microwave Theory and Techn.*, Vol. 6, No. 3, 308–310, 1958.
41. Altman, C. and K. Suchy, *Reciprocity, Spatial Mapping and Time Reversal in Electromagnetics*, Kluwer, Dordrecht, 1991.
42. Lindell, I., A. Sihvola, S. Tretyakov, and A. Viitanen, *Electromagnetic Waves and Bi-Isotropic Media*, Artech House, Boston, 1994.
43. Melrose, D. and R. McPhedran, *Electromagnetic Processes in Dispersive Media*, Cambridge University Press, Cambridge, 1991.
44. Landau, L. and E. Lifshitz, *Electrodynamics of Continuous Media*, Pergamon Press, New York, 1994.
45. Van, Manen, D.-J., J. Robertsson, and A. Curtis, "Modeling of wave propagation in inhomogeneous media," *Phys. Rev. Lett.*, Vol. 94, No. 16, 164301-1–164301-4, 2005.
46. Wapenaar, K., "General wave field representations for seismic modeling and inversion," *Geophysics*, Vol. 72, No. 5, SM5–SM17, 2007.
47. Shen, J., "Negative refractive index in gyrotropically magneto-electric media," *Phys. Rev. B*, Vol. 73, No. 4, 045113, 2006.
48. Kiehn, R., G. Kiehn, and J. Roberds, "Parity and time-reversal symmetry breaking, singular solitons, and Fresnel surfaces," *Phys. Rev. A*, Vol. 43, No. 10, 5665–5671, 1991.